A Numerical Study on the Transition of a Laminar Flame to a Turbulent Flame in a Divided Combustion Chamber

I.S.Jeung, K.K.Cho and S.W.Choi

Department of Aeronautical Engineering
Seoul National University
Seoul 151-742
Korea

ABSTRACT

An attempt was made to simulate the unsteady flame propagation in a divided combustion chamber having dual opposed prechambers by using a numerical analysis. The combustion process in such a chamber is a complex phenomenon in which a laminar flame propagation, the transition of a laminar-turbulent flame, and a fully turbulent flame exist together.

We overcame this problem by introducing reduced β transformation, a kind of artificial flame thickening transformation, which consists with the original β transformation but β_r is automatically reduced wherever the turbulent property increases. By the use of reduced β transformation the flame propagation in this divided combustion chamber was successfully simulated with a rather coarse grid.

Pressure history, temperature, velocity and *NO* species concentration were examined. And they were compared with the results of experiments.

INTRODUCTION

When a premixed flame propagates by or through an obstacle, it is accelerated and becomes turbulent. This is very important phenomenon in flame quenching[1], fire[2] and pollutant formation control in an internal combustion engine[3]. As they are the complicatedly mixed phenomena of an unsteady laminar flame, a transition of a laminar flame to a turbulent flame, and a turbulent flame, it is very hard to understand the details through experiments and numerical simulations.

Recently developed numerical methods have made it feasible to solve two dimensional unsteady conservation equations with sufficient numerical precision. The accuracy of the computed results are determined mostly by the submodels for the controlling processes. The answers can be proved correct only when they are compared with those of equally detailed experiments which, until recent time, have been very scarce.

Here, a simulation for the transition of a laminar flame to a turbulent flame in a divided combustion chamber with dual opposed prechambers was attempted with CONCHAS-SPRAY computer code[4] modified to include the reduced β transformation. Temperature, velocity and *NO* species distribution in the combustion chamber were examined. And it was compared with the results of experiments.

EXPERIMENTS

For the purpose of obtaining data to verify numerical simulation, experiments have been done using a combustion chamber with dual opposed prechambers as shown in Fig. 1. The combustion chamber is of rectangular shape for the convenience of visualization. The dimension of the main chamber was 50 × 50 × 150 *mm*. The volume of each prechamber was 20 % that of the main chamber in volume, and the diameters of connecting orifices were 10 *mm*. Experiments have been done using a 3.8 % propane-air premixture. Ignition has been occurred in each prechamber at the same time. High speed schlieren pictures were taken to visualize the flame propagation processes through glass windows forming side-walls. And the chamber pressure was measured throughout the whole combustion period.

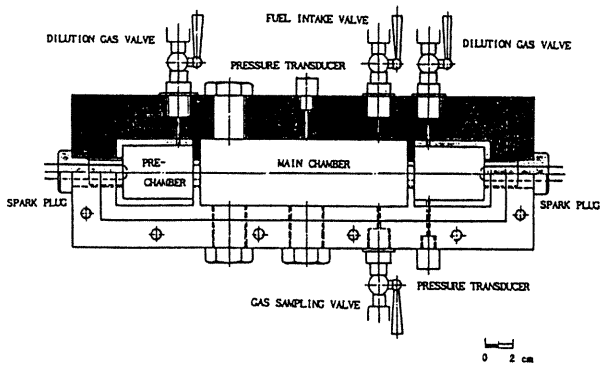

Fig.1. A divided combustion chamber having dual opposed prechambers

GOVERNING EQUATIONS

In experiments, flame propagation is a three dimensional phenomenon. However, most parts of combustion process, i.e. the jet flow issuing from the prechambers through orifices and combustion in the main chamber except the region near the edge, really occur in axisymmetric manner. So in the present study, two dimensional axisymmetric governing equations were solved for convenience.

Chemical species conservation equation

$$\frac{\partial \rho_k}{\partial t} + \frac{1}{R}\nabla\cdot(R\rho_k \mathbf{u}) = \frac{1}{R}\nabla\cdot[R\rho D\nabla(\rho_k/\rho)] + \dot{\rho}_k^C \qquad (1)$$

where, $\rho = \sum_k \rho_k$, $\dot{\rho}_k^C = W_k \sum_r (b_{kr} - a_{kr})\,\dot{\omega}_r$,

Mass conservation equation

$$\frac{\partial}{\partial t}(\rho \mathbf{u}) + \frac{1}{R}\nabla\cdot(R\rho\mathbf{u}) = 0 \tag{2}$$

Momentum conservation equation

$$\frac{\partial}{\partial t}(\rho \mathbf{u}) + \frac{1}{R}\nabla\cdot(R\rho\mathbf{u}\mathbf{u}) = -\nabla p + \frac{1}{R}\nabla\cdot(R\sigma) - \frac{\sigma_0}{R}\nabla R \tag{3}$$

$$\text{where, } \sigma = \mu[(\nabla\mathbf{u}) + (\nabla\mathbf{u})^T] + (\lambda/R)\nabla\cdot(R\mathbf{u})\mathbf{I}_d$$

$$\sigma_0 = (2\mu/R)\mathbf{u}\cdot\nabla R + (\lambda/R)\nabla\cdot(R\mathbf{u})$$

Energy conservation equation

$$\frac{\partial}{\partial t}(\rho I) + \frac{1}{R}\nabla\cdot(R\rho I\mathbf{u}) = -\frac{P}{R}\nabla\cdot(R\mathbf{u}) + \frac{\sigma_0}{R}\mathbf{u}\cdot\nabla R - \frac{1}{R}\nabla(R\mathbf{J}) + \dot{Q}_C \tag{4}$$

$$\text{where, } \mathbf{J} = -K\nabla T - \rho D\sum_k h_k \nabla(\rho_k/\rho)$$

$$\dot{Q}_C = \sum_r q_r\dot{\omega}_r, \quad \nabla = \mathbf{i}\frac{\partial}{\partial R} + \mathbf{j}\frac{\partial}{\partial Z}$$

State equations of ideal gases

$$P = R_g T \sum_k (\rho_k/W_k) \tag{5}$$

$$h_k(T) = I_k(T) + R_g T/W_k \tag{6}$$

$$I(T) = \sum_k (\rho_k/\rho) I_k(T) \tag{7}$$

$$C_v(T) = \sum_k (\rho_k/\rho) C_{vk}(T) \tag{8}$$

These equations are appropriate to laminar flow, so a modification is needed to be able to treat turbulent flow. For averaging, all the flow variables were decomposed into mean and fluctuating components, and mean values were mass weighted (so called Favre averaging). After these processes, the averaged equations have the same form as the laminar ones. Only the transport coefficients are replaced by appropriate values that have turbulent contributions added to the laminar values. They are calculated from the following equations.

$$\mu = \mu_l + \mu_t$$

$$K = C_p \mu / Pr = \mu C_v (9\kappa - 5)/4 \tag{9}$$

$$D = \mu/(\rho Sc) = \mu(9\kappa - 5)/(4\rho\kappa Le)$$

where, laminar viscosity coefficient $\mu_l = 1.457\times10^{-5} T^{3/2}/(T + 110K)$ (g/cm·s), μ_t represents turbulent viscosity coefficient calculated using SGS submodel [5], Pr is the Prandtl number which calculated from the Eucken formula [6], Sc is the Schmidt number (Sc = Pr ×Le), and Le is the Lewis number (= 1.0).

CHEMICAL REACTIONS

In the present study, propane-air premixture of 3.8 % volumetric mixture ratio was used. For the calculation of heat release by combustion, one-step global chemical kinetics of propane was considered instead of adopting detailed elementary reaction kinetics, which is a time-consuming procedure. It was assumed that 12 chemical species take part in the chemical reactions. Four kinetic reactions and six equilibrium reactions were considered.

One-step global kinetic reaction

$$C_3H_8 + 5O_2 + 18.8N_2 \rightarrow 3CO_2 + 4H_2O + 18.8N_2 \tag{10}$$

Extended Zel'dovich reaction kinetics

$$\begin{aligned} &O + N_2 \rightleftarrows NO + N \\ &N + O_2 \rightleftarrows NO + O \\ &OH + N \rightarrow NO + H \end{aligned} \tag{11}$$

Equilibrium reactions

$$\begin{aligned} &H_2 \rightleftarrows 2H \qquad O_2 \rightleftarrows 2O \\ &N_2 \rightleftarrows 2N \qquad O_2 + H_2 \rightleftarrows 2OH \\ &O_2 + 2H_2O \rightleftarrows 4OH \qquad O_2 + 2CO \rightleftarrows 2CO_2 \end{aligned} \tag{12}$$

Kinetic reaction coefficients were assumed to be Arrhenius type as an example shown for the one-step propane oxidation reaction kinetics

$$\dot{\omega} = A\exp\left[-\frac{E^+}{T}\right]\left[C_3H_8\right]^a\left[O_2\right]^b \tag{13}$$

where, reaction coefficient $A = 2\times10^7$cc/mol/sec, activation temperature $E^+ = 14000$K, and reaction order a=b=0.5 were used for propane.

ARTIFICIAL FLAME THICKENING

In numerical calculation of the propagating flame, one usually finds that the flame thickness which we want to deal with is much thinner than the computing cell size. Therefore a large computer capacity is required to retain spatial resolutions suitable for either thin laminar flame or rather thicker turbulent flame, which exist simultaneously in the combustion chamber. Butler and O'Rourke introduced a coordinate stretching technique [7], called β-transformation [8], that broadens the flame front, thus facilitating its numerical computation greatly.

This study, however, involves two additional difficulties in numerical computation originated from the small characteristic scale at the orifice region and from the complexity of the combustion processes in the divided combustion chamber where a laminar flame, the transition of a laminar-turbulent flame, and a fully turbulent flame exist together. Consequently the application of β-transformation is no longer said to be valid because it was originally developed on the assumption that the whole flame propagation is a laminar or near laminar flame propagation and that the shortest characteristic length in the flow field is much larger than the stretched flame thickness. We overcame this

problem by introducing an artificial flame thickening transformation as follows. Basically this transformation consists with the original β-transformation proposed by O'Rourke and Bracco [8], which scales up the diffusivity by a factor of β_r while reducing the reaction rate by a factor of β_r. But β_r is automatically reduced wherever the turbulent property increases.

The reduced β-transformation used is given as

$$\beta_r = \frac{\beta_o \mu_l + \mu_t}{\mu_l + \mu_t} \qquad \lim_{\mu_t \to 0} \beta_r = \beta_o, \quad \lim_{\mu_t \to \infty} \beta_r = 1 \tag{14}$$

$$\text{where, } \beta_o = \max[1, \frac{c\Delta X^2}{\delta} \frac{|\nabla T|}{\Delta T}]$$

c(=4) is the number of cells over which the flame is to be spread, and δ (=0.1mm) is the true flame thickness, ΔT (=2000 K) is the temperature jump across the flame, and ΔX is the characteristic length of a cell.

COMPUTATIONAL GRID AND BOUNDARY CONDITIONS

To obtain a solution of two-dimensional governing equations, combustion chamber shape was simplified to a cylinder of equivalent volume. The radii of main chamber and prechamber are 56 *mm* and 44 *mm* respectively and axial lengths of main chamber and prechamber were 148 *mm* and 50 *mm* respectively to meet the volume ratio 0.2 of the prechamber to the main chamber. The diameters of connecting orifices were 12 *mm* for uniform grid distribution.

Considering the axial symmetry, we selected a cross sectional plane containing the axis of symmetry as a computational domain. And by using the symmetry of dual opposed-prechambers, computation has been done in its 1/4 domain as shown in Fig. 2. Computational domain was equally divided into 14 and 65 in radial and axial directions respectively.

Numerical ignition was performed at eight cells adjacent to experimental ignition point, which is located 5 *mm* from prechamber end-wall along the center line, by deposing energy until the temperature becomes 1600 K.

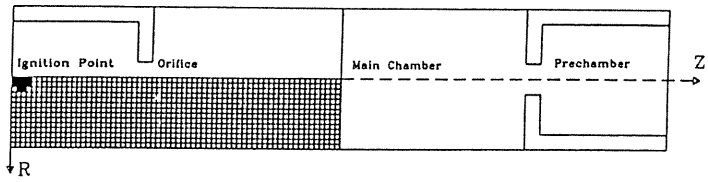

Fig.2. Computational Domain and grid system

Slip and adiabatic boundary conditions were applied along the symmetry line. And at combustion chamber wall, law-of-the-wall condition for the flow velocities and constant wall temperature condition were applied. In the constant temperature wall boundary condition, two kind of test runs were made.

Case 1 is considering turbulent thermal boundary layer which is an appropriate simplification of a formula proposed by Launder and Spalding [9]

$$q = 1.125(\frac{\tau}{u})C_P(T - T_w) \tag{15}$$

Case 2 is not considering existence of thermal boundary layer

$$q = K\frac{\partial T}{\partial X} = K\frac{(T - T_w)}{\Delta X} \tag{16}$$

where K is the thermal conductivity given by Eq (9). In the computation process, flame quenching is not appropriately considered. So by applying the constant wall temperature conditions, heat loss to the walls could give the similar effect as flame quenching near the wall.

RESULTS AND DISCUSSIONS

In numerical calculation of the cases similar to this study, if one uses original β-transformation proposed by O'Rourke and Bracco [8], one can simulate the near laminar flame propagation in the prechamber regions but fails to simulate the transition of

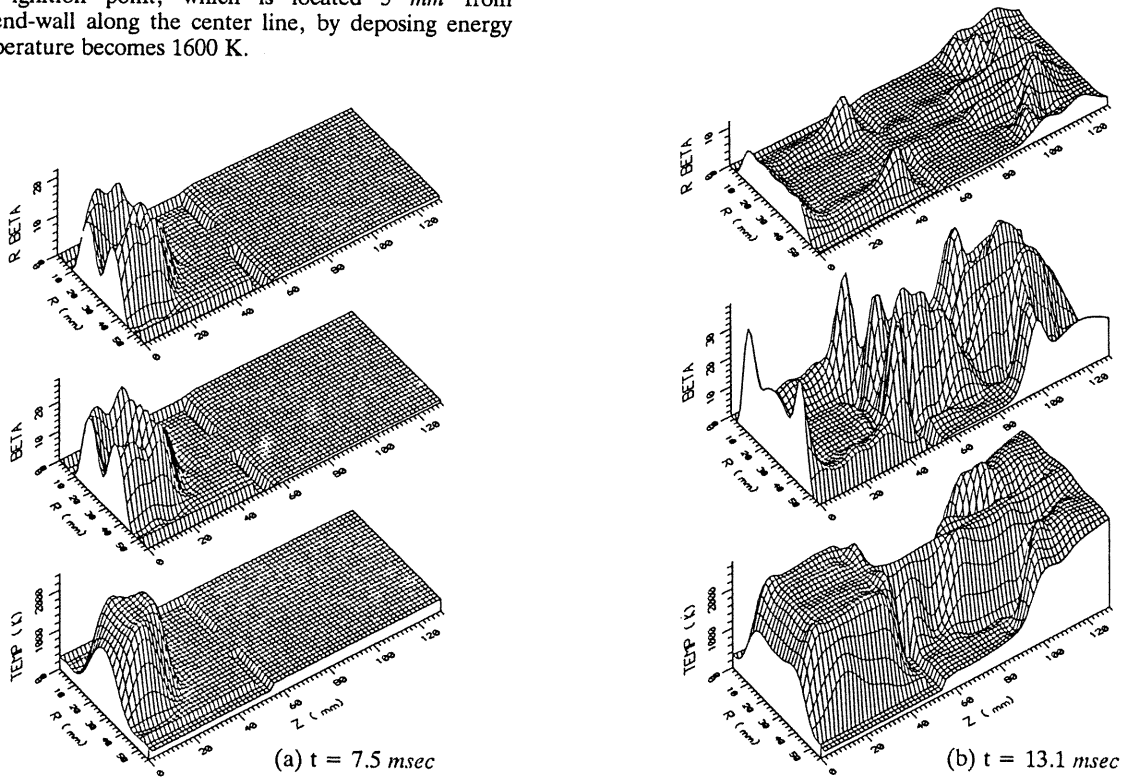

(a) t = 7.5 *msec* (b) t = 13.1 *msec*

Fig.3. Comparision of original β-transformation and reduced β- transformation
(a) t = 7.5 *msec* (b) t = 13.1 *msec*

laminar-turbulent flame propagation through the orifice, i.e., flame does not propagate any longer or is cut by flame stretching (while in experiment, flame propagates with the transition of a laminar-turbulent flame through the orifice and propagates to a fully turbulent flame in the main chamber). So, one can find that original β-transformation is no longer valid in this case study.

And if one assumed that entire computational domain was fully turbulent region, i.e., used large turbulent diffusivity [7], one still met numerical ignition difficult, and the flame propagation in the prechamber did not agree with that of experiment. We calculated both cases mentioned above and confirmed previously mentioned comments, but we do not report theirs in this paper.

We can overcome this problem by introducing reduced β-transformation which consists with the original β-transformation but β_r is automatically reduced wherever the turbulent property increases.

The effectiveness of the reduced β-transformation is demonstrated in Fig.3 typically on the time at $t = 7.5msec$ and $t = 13.1msec$, the former illustrating the laminar flame propagating inside the prechamber, while the latter illustrating the turbulent spouting jet flame propagating inside the main chamber also inside the prechamber. Fig.3(a) shows that both results of original β-transformation and reduced β-transformation are quite similar to each other. But in Fig.3(b) reduced β-transformation has very small values than those of original β-transformation, where the turbulent flame is dominating through the whole flow field of the combustion chamber. This reduced value can induce the effects of the turbulences, which usually promote the chemical reactions within the flame zones.

Results of computation depend heavily on boudary conditions assigned. In this study, turbulent law of the wall condition for the flow velocity and constant temperature wall boudary conditions were applied. Regarding thermal boudary layer, two kinds of test runs were made. One is considering turbulent thermal boundary layer which is an appropriate simplification of a formula proposed by Launder and Spalding[9], and the other not considering existence of thermal boundary layer.

The accuracy of simulated results were deductively verified by comparing pressure history with that of experiment. The pressure history was given in Fig.4. When the turbulent thermal boundary layer stated above was assumed to exist (Case 1), pressure starts to rise earlier than experiment, and peak pressure reaches as high as 9 atm such can be obtained when adiabatic wall condition is applied. With these results, it can be considered that assumed thermal boundary layer was not proper. This seems to result from the lack of knowledges on the quenching mechanisms near the wall. The gases near the wall that quenched in experiments are burnt in computation. Hence it was assumed that thermal boundary layer does not exist (Case 2). Then the pressure history shows closer trend in starting time of pressure rise and in the magnitude of peak pressure. And in this case, sufficient heat was transferred through the wall by calculating heat flux using the difference between the wall and nearest grid points. It seems that overestimated heat loss results in the same effect as quenching near the wall. But after the time 12 *msec*, when the turbulent combustion in the main chamber occurs, the computational pressure history is somewhat inconsistent with that of experiment. It may be due to the lack of informations on the quenching effect, turbulent modeling in combustion and uncertainty of applied chemical kinetics data for the turbulent combustion.

Fig.5 shows the averaged temperature, the averaged *NO* concentration after the ignition till end of the whole combustion process, and the measured NO_x concentration in experiment.

Considering the relationship between the averaged temperature and the amount of *NO* product, Fig.5 shows that *NO* is appearently produced when the averaged temperature rises up to 1200 K, and that the rate of *NO* product increases as the averaged temperature increases till near maximum averaged temperature where the inflection point of the curve of *NO* product has occured. And as the averaged temperature downs below a certain temperature (1800 K, in Case 2), *NO* formation is nearly frozen. In the case of applying thermal boundary layer (Case 1) like near adibatic condition, inflection point of the curve of *NO* product appears at the near maximum averaged temperature, but *NO* is continuously produced long after the time when the maximum averaged temperature was indicated, and the amount of *NO* formation is inordinately larger than that of experiment. This is due to the effect of long residence time exposed in the high temperature burnt gas region. While in Case 2, the amount of *NO* formation is fairly good agreement with that of experiment.

Visualized flame propagation and simulated flow velocity field and isothermal lines at selected times for Case 2 are shown in Fig.6. Temperature gradient in the flame front is so steep that the densely distributed isothermal lines can be regarded as flame front, which makes it relatively easy to compare the flame position with that of schlieren photographs.

Flame propagates like nearly laminar flames propagation in the prechamber region. As flame approaches the orifice,

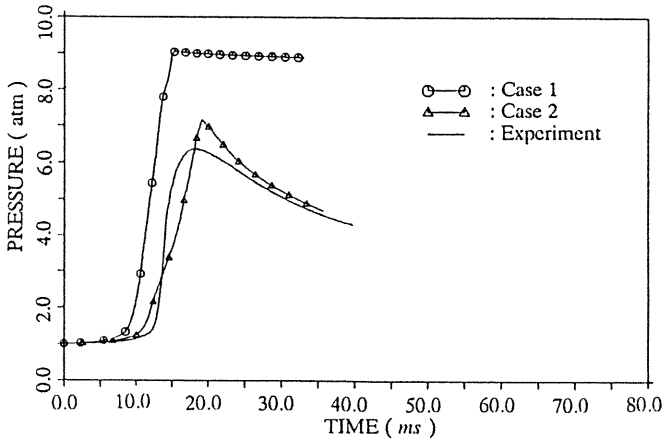

Fig.4. Pressure history of combustion chamber
(a) Case 1; including thermal boundary layer
(b) Case 2; excluding thermal boundary layer

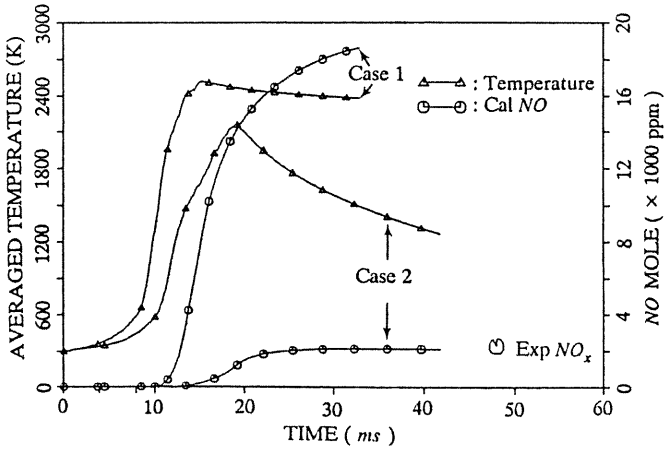

Fig.5. Averaged temperature history and *NO* formation history
(a) Case 1; including thermal boundary layer
(b) Case 2; excluding thermal boundary layer

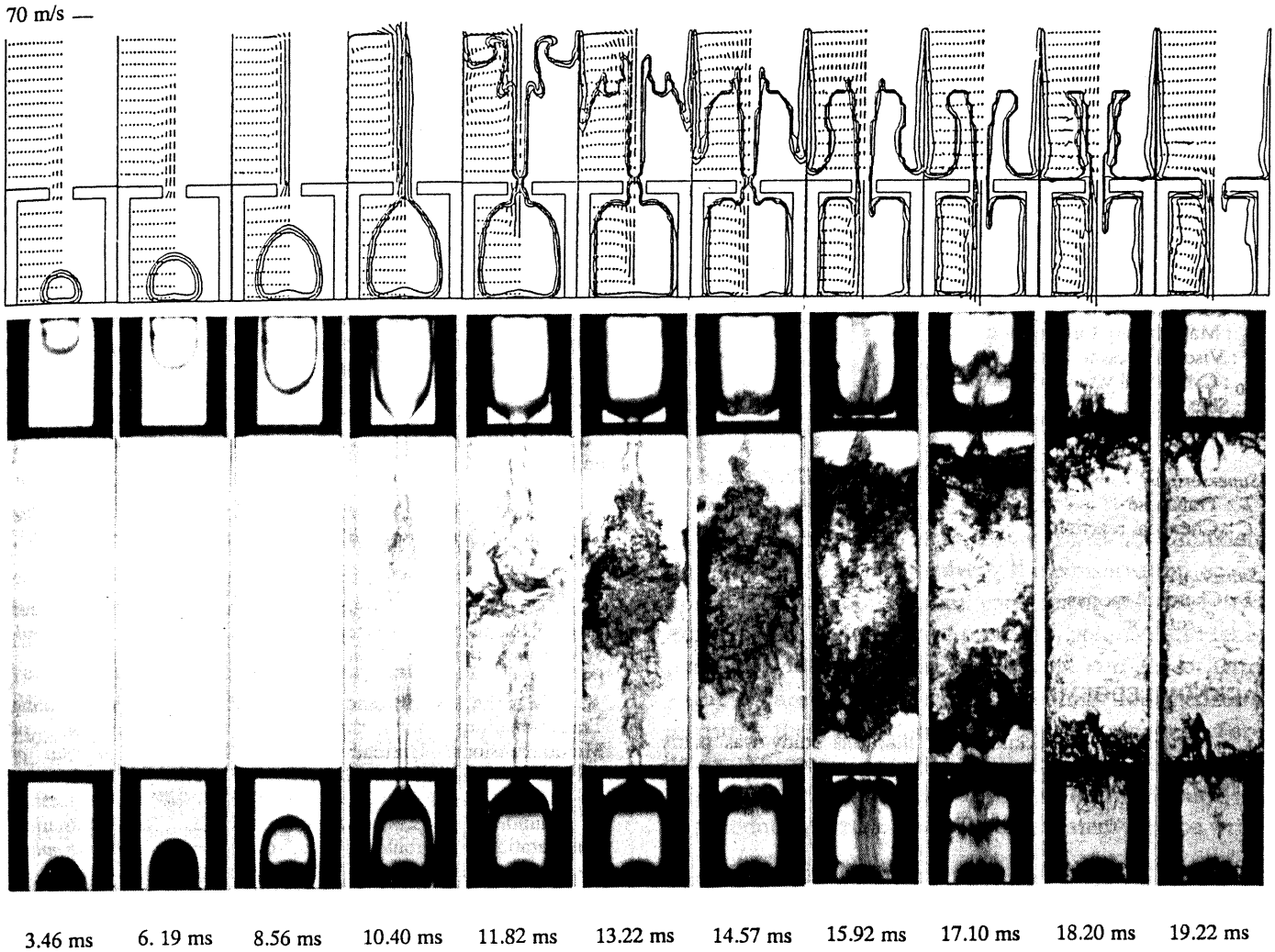

Fig.6. Velocity vector field and isothermal lines compared with the Schlieren pictures at some selected steps

transition from a laminar flame to a turbulent flame begins to occur. Finally fully turbulent flame propagation is observed in the main chamber.

As a whole, computation simulates the phenomena fairly well, but still leaves room for improvement on the modeling of turbulent combustion in the main chamber after jet issuing. It may be due to turbulent modeling and chemical kinetics data etc., which call for further studies.

CONCLUDING REMARKS

Measurements and simulation of combustion have been made in a divided combustion chamber having dual opposed prechambers, and they were compared at selected times. Reduced β transformation enabled us to calculate the transition from a laminar flame to a turbulent flame numerically with a rather coarse grid. Referenced to the thermal boundary layer, the case of neglecting the existence of thermal boundary layer near the wall gave better results than that of considering it with a rather coarse grid. Pressure history, *NO* concentration, and flame propagation phenomena could be simulated closely with the experiment by use of modified CONCHAS-SPRAY code on the whole. But on some problems like the turbulent combustion in the main chamber after jet issuing and maximum pressure inconsistence are left room for improvement. These may be due to the lack of informations on the quenching effect, turbulent modeling and chemical kinetics data, so further studies will be required.

NOMENCLATURE

Alphabetics

A : pre-exponential factor
a, b : Dimensionless stoichiometric coefficients
C_p : Specific heat at constant pressure (cell quantity)
C_v : Specific heat at constant volume (cell quantity)
C_{vk} : Specific heat at constant volume for species k
D : Species diffusivity (assumed the same for all species)
E^+ : Activation temperature
h_k : Partial specific enthalpy for species k
$\mathbf{I}_d$: Unit dyadic tensor
I : Internal energy
I_k : Partial specific internal energy for species k
$\mathbf{J}$: Heat flux vector
K : Thermal conductivity
P : Pressure
Q : Heat of chemical reaction
Q_C : Rate of chemical heat release
q : Heat flux through the wall
q_r : Negative of the heat of reaction for r^{th} reaction
R : R coordinate
R_g : Universal gas constant
T : Temperature

T_w : Wall temperature
t : Time
$\mathbf{u}$: Velocity vector
W_k : Molecular weight of species k
Z : Z coordinate

Greeks
β_o : Coefficient of β transformation
β_r : Coefficient of reduced β transformation
δ : flame thickness
ΔX : characteristic length of cell
κ : specific heat ratio
μ : First viscosity coefficient
ρ : Total mass density
ρ_k : Mass density for species k
σ : Viscous stress tensor
σ_0 : Cylindrical viscous stress
τ : Shear stress
$\dot{\omega}_r$: Reaction rate of r^{th} reaction

Superscripts
T : Transpose
C : Chemical reaction

Subscript
k : Chemical species
r : r^{th} reaction

ACKNOWLEDGEMENT

Authors wish to acknowledge that this study was partly supported by a Grant-in-Aid of fiscal year 1989 (Subject No 890203) from Korea Science and Engineering Foundation.

REFERENCES

1. Beretta, G. P. and Jarosinski, J., "Flame Quenching by Turbulence," *Combustion and Flame*, Vol.48, pp.241-249, 1982.

2. Brandeis, J., "Effects of Obstacles on Flames," *Combustion Science and Technology*, Vol. 44, pp.61-73, 1985.

3. Fujimoto, S., Kaneko, Y., and Tsuruno, S., "Possibility of Low-NO_x and High-Load Combustion in Premixed Gases," *Twentieth Symposium (International) on Combustion*, pp.61-66, 1984.

4. Cloutman, L. D., Dukowicz, J. K., Ramshaw, J. D. and Amsden, A. A., "CONCHAS - SPRAY : A Computer Code for Reactive Flows with Fuel Sprays," *Los Alamos Scientific Laboratory Report LA-9294-MS* , 1982.

5. Deardorff, J. W., "On the Magnitude of the Subgrid Scale Eddy Coefficient," *Journal of Computational Physics* , Vol.7, pp.120-133, 1971.

6. Williams, F. A.,"Combustion Theory," *2nd edition, The Benjamin / Cummings Publishing Company, Inc*, pp.642-647, 1985.

7. Butler, T. B. and O'Rourke, P. J., "A Numerical Method for Two Dimensional Unsteady Reacting Flows," *Sixteenth Symposium (International) on Combustion*, pp.1503-1515, 1976.

8. O'Rourke, P. J. and Bracco, F. V., " Two Scaling Transformations for the Numerical Computation of Multidimensional Unsteady Laminar Flames, " *Journal of Computation Physics*, Vol. 33, pp 185-203, 1979.

9. Launder, B. E. and Spalding, D. B. ,"The Numerical Computation of Turbulent Flows," *Computer Methods in Applied Mechanics and Engineering*, Vol.3., pp.269-289, 1974.